From path models to commands during additive printing of large-scale architectural designs

IOP Conf. Series: Journal of Physics: Conf. Series **1015** (2018) 032020 doi:10.1088/1742-6596/1015/3/032020

From path models to commands during additive printing of large-scale architectural designs

M S Chepchurov[1], E M Zhukov[1], E A Yakovlev[1] and V G Matveykin[2]

[1] Belgorod State Technological University named after V. G. Shukhov, Belgorod, 308012, Russia
[2] Tambov State Technical University, 106, Sovetskaya St., Tambov, 392000, Russia

E-mail: avtpost@mail.ru, chepchurov.ms@bstu.ru

Abstract. The article considers the problem of automation of the formation of large complex parts, products and structures, especially for unique or small-batch objects produced by a method of additive technology [1].
Results of scientific research in search for the optimal design of a robotic complex, its modes of operation (work), structure of its control helped to impose the technical requirements on the technological process for manufacturing and design installation of the robotic complex. Research on virtual models of the robotic complexes allowed defining the main directions of design improvements and the main goal (purpose) of testing of the the manufactured prototype: checking the positioning accuracy of the working part.

1. Introduction

Formation methods of large complex parts [2], products and structures, especially for unique or small-batch objects are critical in the modern market conditions, because they determine configuration, dimensions and quality indicators of the final product. Speeding-up of design and prototyping of a future product, as well as production of process gear for formation of components, are becoming especially timely tasks. [3]. To resolve the task, a decision was made to design an experimental sample of a robotic complex (RC) to implement full-scale additive technology with innovative materials [4, 5].

2. Main part

Determining the coordinate system. Movement trajectory of the end-effector of the RC is built in a single selected coordinate system [6], to which all the movements of units, elements and mechanism of the robotic complex are fixed [7]. Figure 1 shows a diagram of an overhead manipulator-based RC. The diagram shows foundation 1, which supports rail track 2 with 6000 mm gage, where portal 3 is moving, which serves as the base of the robotic complex and its main support structure. The foundation may be provided with a special platform, serving as a base to fabricate a product by layering the construction mixture. At that, the platform shall be able to move on its own in parallel to the portal to remove the product from the formation zone. Portal 3 of the RC is provided with horizontal platform 4 with an ability of vertical movement along the axis which is strictly orthogonal to the plane of the foundation 1. On platform 4 there is bridge 5, moving in parallel to the direction of portal movements or to rail track 2; at that, the bridge is provided with a precision drive for exact positioning in the horizontal plane.

Bridge 5 is provided with carriage 6, moving in the direction perpendicular to that of the bridge. The carriage is provided with end-effector 7. In the variant of RC shown in Figure 1, end-effector is a cylinder provided with a nozzle that forms a stack of material for laying down. The mixture may be supplied from an external source as well, but in any case, the nozzle shall form the plastic stack of the material.

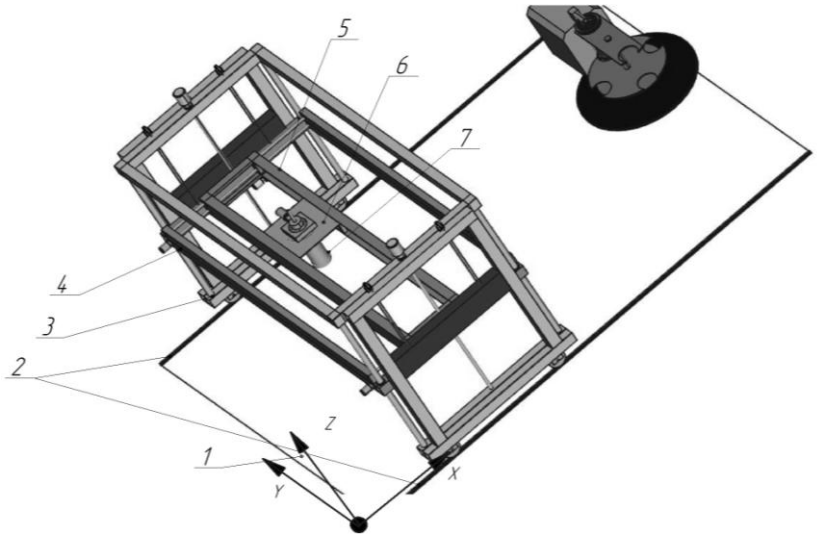

Figure 1. A diagram of a robotic complex based on an overhead manipulator.

The RC coordinate system composed is shown in Figure 2 and has three degrees of freedom: X_b; Y_b: Z_b. It is the main or basic coordinate system, linked to the foundation of the model shown in Figure 1. On the foundation, there is a working platform intended for product formation, it has its own coordinate system: X_{pj}; Y_{pj}: Z_{pj}. The product being formed on the platform has its own coordinate system: X_{pt}; Y_{pt}; Z_{pt}. Thus, to determine coordinates of the product in the coordinate system, one shall use expression 1, where corresponding designations of the coordinates are given [8, 9]:

$$\begin{cases} X_{pd} = X_{0pj} + X_{0pt} \\ Y_{pd} = Y_{0pj} + Y_{0pt} \\ Z_{pd} = Z_{0pj} + Z_{0pt} \end{cases}, \quad (1),$$

where X_{0pj}; Y_{0pj}; Z_{0pj} is a displacement of the working platform coordinates with respect to the origin of the foundation coordinate system, mm; X_{0pt}; Y_{0pt}; Z_{0pt} is a displacement of the product coordinate system origin from the origin of the working platform coordinate system.

The portal has only one axis of displacement with respect to the basic coordinate system (that of foundation): Y_p; at that, its movements are coarse, but nevertheless, they are taken into account when moving the end-effector. The amount of this displacement we will designate as Δp, it may has either a negative, or a positive direction. The bridge may also move along the basic axis Y_b, changing the Y_{cr} coordinate factoring in the parameter Δp; accuracy of bridge positioning and that of other components is significantly lower than the allowance values of the final product, thus, they may be dismissed during the calculations. As per formula 2, location of the end-effector coordinate system along the Y axis is determined with:

$$Y\_c = Y\_p + Y\_cr \pm \Delta p , \quad (2)$$

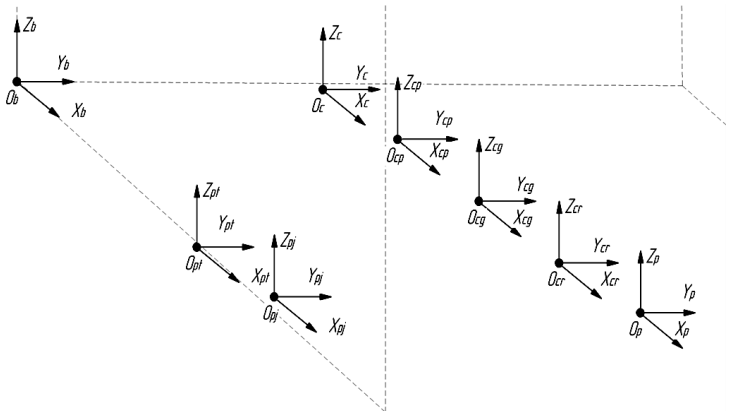

Figure 2: RC coordinate system

However, Δp is constant, as the portal assumes a rigid fixation in a given position.

The carriage with the end-effector is equipped for accurate movements along the X axis, that is, the final position of the end-effector along the axis is determined with formula 3:

$$X\_c=X_p+X_{0cg}, \quad (3)$$

where X_{0cg} is a displacement of the carriage coordinate system with respect to the basic coordinate system.

A similar expression is given for vertical movements along the $Z=Z_p$ axis, that is, setting of the end-effectors is performed with the platform alone.

Movements along the Z axis are performed only when switching to the next layer, the profile of the product is formed in the XY plane. Step of the platform along the vertical axis is linked only to the process parameters, as it is defined by the required thickness of the layer, which in its turn, is defined by rheological properties of the material and is determined experimentally [10].

Routing the end-effector movement. Movement of the end-effector in the XY plane may have either linear or circular trajectory [1, 12, 13].

A feature of the end-effector trajectory generation is that the trajectory is an axis of a stack being formed by the nozzle out of the building material, as it is shown in Figure 3, but only for movements along the X axis with the speed of v.

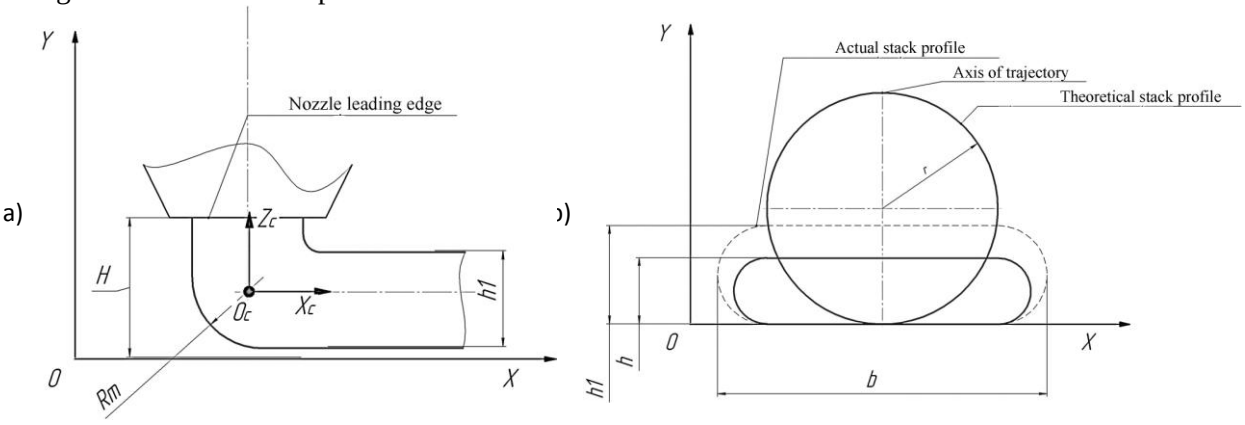

Figure 3. A diagram of material placement along the trajectory: a – stack profile formation in the transverse direction; b – stack formation in the longitudinal direction.

An ideal layering with a circular profile of radius r is when nozzle height H is determined by radius R; however, due to plasticity (plastic flow) of the material, it is impossible, because the material of the stack subside to a height h, at that, the stack being formed has a width of b. When the material solidifies, it contracts as it is defined by its properties, at that, the stack width changes to $b_1=k_y \cdot b$,

where k_y is the contraction coefficient of the material. This implies that when the end-effector trajectory changes, a flaw may arise on the trajectory: disruptions or deposits of the stack material. The proposed variants for trajectory rotation are shown in Figure 4.

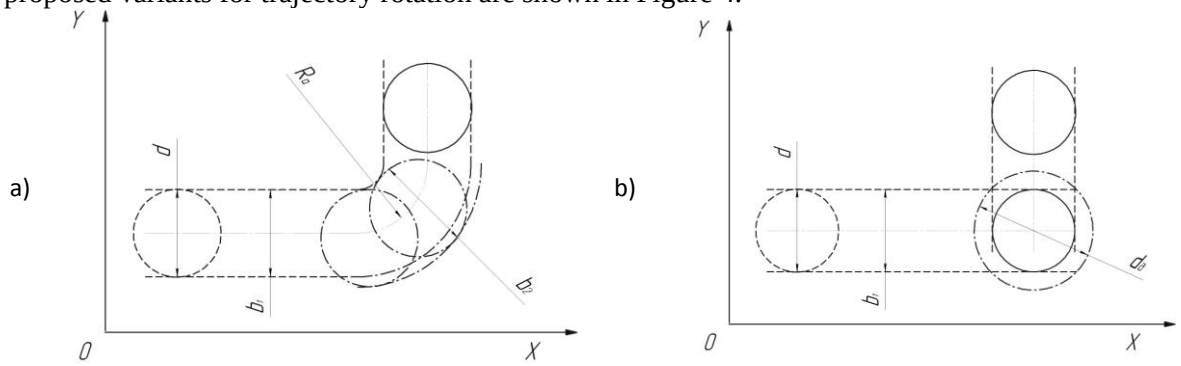

Figure 4. Variants for change of direction on a trajectory: a – angular; b – radial

In the angular variant of the trajectory formation, there is an abrupt change. At that the end-effectors shall stay at the tipping point for some time, for in this point a change of drive speed along the axes take place, or the direction of the displacement vector changes. So, it is necessary either to stop the feeding of material, or to take into account the defect formation in the material stack, a deposit with a diameter d_∂. That is, feeding of additional material to the tipping point, the additional volume is determined as: $V_m = v_m \cdot F \cdot t$, mm^3, where v_m is the material feeding speed, mm/s, F the sectional area of the nozzle, mm^2, t is the stop time, s.

In the radial change of the end-effector trajectory, when the radius of trajectory reduces, there is an overlay of material at the turn location. At that, one should assess the changes in stack thickness depending on the turn radius R_a: the larger the bend radius is, the less the width b_2 and the distortion in the stack profile and trajectory are, and vice versa.

The trajectory is divided into sections, determined by interpolation, at that, only two types are distinguished: linear and circular interpolation, a graphical representation is shown in Figure 5. In linear interpolation, the displacement speed in its vector form: $\vec{v} = \overrightarrow{v_x} + \vec{v}_y$, in case $\overrightarrow{v_x} = max, \vec{v}_y = 0$ and $\overrightarrow{v_x} = 0, \vec{v}_y = max$, that is, the end-effector is moved only along one of the axes [14].

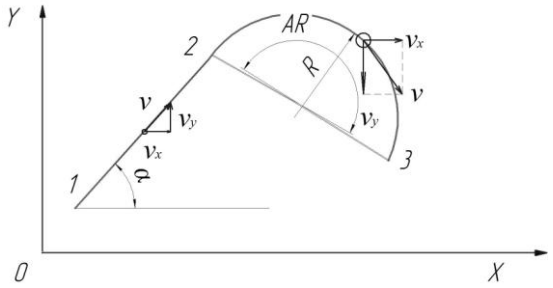

Figure 5. Trajectory formation for the end-effector displacement with sections of various interpolation types

Thus, the end-effector displacement rate between point 1 and point 2 may be defined as $v = \sqrt{v_x^2 + v_y^2}$. At that, the path along each of the axes is determined as $x_2 - x_1$ и $y_2 - y_1$, where x and y are the coordinates, time to perform the displacement along each of the axes is $t_{x1\text{-}2} = t_{y1\text{-}2}$. Thus, it may be concluded that in linear displacement along each of the axes, synchronization of changes in speed allows one to completely avoid interpolation of their trajectory, that is, a stepped form. The ratio of speeds may be expressed and tangent of the trajectory tilt angle with respect to the X axis is

$\tan\alpha = \frac{|y_2-y_1|}{|x_2-x_1|}$, or $\tan\alpha = \frac{|v_y|}{|v_x|}$, which is enough for control over the drives. According to Figure 5, the speed vector is always directed along the normal line to the radius of the stack obtained; only the value of aperture angle AR change, thus, its monitoring allows one to determine the values of speed in each point of the trajectory. From Figure 7, $v_x = v \cdot cos(90 - AR)$, $v_y = v \cdot sin(AR)$, thus, by monitoring changes in AR from min to max, one may calculate changes of speed along each of the axes at any point of the circular trajectory. The step of the AR angle is the interpolation step, at that, a change in the angle may be assigned by a certain function AR=f(t), that is, the angle will change during the period from t_2 to t_3 from its initial value to the final value, thus, serving as a path identifier for a known radius R [15].

The final model of the additive manufacturing end-effector displacement for the time criterion has the following form: having divided the sections with linear and circular interpolation, for the linear interpolation:

$$T_l = \sum_{i=1}^{n} \frac{\sqrt{(x_i - x_{i-1})^2 + (y_i - y_{i-1})}}{v_i}, \text{ min}, \quad (4)$$

where i is the number of a trajectory section; v_i is respectively a speed at the i-th section of the trajectory, m/min.

For the circular interpolation:

$$T_c = \sum_{i=1}^{n} \frac{\pi R_i AR_i}{v_i \cdot 360}, \text{ min}, \quad (5)$$

where R_i is a radius of a corresponding circular section in the same units of measure as the coordinates; AR_i is the aperture angle of the circular section.

Putting expressions 4 and 5 together for presence of any types of interpolation, one obtains:

$$T = \sum_{i=1}^{n} \left(\frac{\sqrt{(x_i - x_{i-1})^2 + (y_i - y_{i-1})}}{v_i} \cdot (1 - |sign(R)|) + \right. \\ \left. + \frac{\pi R_i AR_i}{v_i \cdot 360} \cdot |sign(R)| \right), \text{ min}. \quad (6)$$

It is evident that the value of coordinates for each drive shall be re-calculated in accordance with formulas 2 and 3. At that, parameter v_i is still in the formula 6, for each section, because it is necessary to separate the transitions for laying down the material, and transitions for service movements of the end-effectors [16]. To lay down the material the end-effector is moved at a speed necessary to lay down a required volume of material on the working base surface, thus, knowing the wall thickness of the product being formed, one may calculate the current material consumption per a unit of time [17, 18].

3. Findings

Process parameters of RC functioning are determined for manufacturing of products of various forms and dimensions:

1. A coordinate system of the robotic complex is defined as the foundation coordinate system linked to the local coordinate systems of all the units of the robotic complex and allowing one to obtain the product contour by calculating the ratios of the end displacements along the product coordinate axes.

2. It has been proven that dividing the end-effector displacement trajectory into elementary sections with only two attributes, linear and circular, allows constructing a model of the displacement trajectory, reflecting changes in the coordinates in the plane of the product layer being worked on, thus allowing one to obtain a command line structure for controlling the end-effector displacement, characterized with the minimal set of commands needed to obtain the product contour.

4. Conclusion

An experimental specimen of a robotic complex, manufactured and installed in accordance with the technical requirements, was subjected to testing according to the testing program and procedure developed during this project. According to the test protocol, maximum positioning error of the RC end-effector amounted to 0.24 mm, which satisfies the conditions of the technical design specification. Thus, the parameters set in the design task were attained during the performance of the works.

5. Acknowledgments

The article was prepared within development program of the Flagship Regional University on the basis of Belgorod State Technological University named after V.G. Shoukhov, using equipment of High Technology Center at BSTU named after V.G. Shoukhov

References

[1] Wohlers T, Campbell I, Diegel O, et al. 2017 3D Printing and Additive Manufacturing State of the Industry. Wohlers Report. *Wohlers Associates*
[2] Johnston DW 1997 Design and construction of concrete formwork. *In E. G. Nawy (Ed.), Concrete construction engineering handbook.* Boca Raton, Fla.: CRC Press., 7.1-740
[3] Yi Wei Daniel Tay, Biranchi Panda, Suvash Chandra Paul, Nisar Ahamed Noor Mohamed, Ming Jen Tan & Kah Fai Leong 2017 3D printing trends in building and construction industry: a review, *Virtual and Physical Prototyping* **12(3)** 261-276
[4] Bechthold M, King N, Kane A, Niemasz J, Reinhart C 2011 Integrated environmental design and robotic fabrication workflow for ceramic shading systems. *In: Proceedings of the 28th international symposium on automation and robotics in construction*. (Seoul, Korea)
[5] Semini C, Baker M, Laxman K, Chandan V, Maruthiram T, Robert Morgan R, Frigerio M, Barasuol V, Caldwell DG, Rey G 2016 A brief overview of a novel, highly-integrated hydraulic servo actuator with additive-manufactured titanium body. *In: IEEE/RSJ IROS workshop on force torque controlled actuation*
[6] GOST R 55021-2012/ISO/IEC TR 9789:1994 2013 *Information Technology. Guidelines for the organization and representation of data elements for data interchange. Coding methods and principles.* (Moscow: Standartinform)
[7] GOST 2.052-2006. *Unified system for design documentation. Electronic Product Model. General provisions* (Moscow: Standartinform)
[8] ISO/ASTM 52921:2013 (ASTM F2921) Standard terminology for additive manufacturing - Coordinate systems and test methodologies
[9] ISO/ASTM 52900-15 Standard Terminology for Additive Manufacturing-General PrinciplesTerminology
[10] Tymrak B M, Kreiger M, Pearce J M 2014 Mechanical properties of components fabricated with open-source 3-D printers under realistic environmental conditions. *Materials and Design*, **58** 242-246
[11] Izard J B, Dubor A, Hervé P E. et al. 2017 Constr Robot *Large-scale 3D printing with cable-driven parallel robots*, **1(1–4)** 69–76
[12] Jewell C 2013 3D PRINTING and the future of stuff, *WIPO magazine*, April 2013, 2-6
[13] Canessa E, Fonda C, Zennaro M 2013 Low-Cost 3D Printing, *ICTP—The Abdus Salam International Centre for Theoretical Physics*
[14] Gopsill J A, Shindler J & Hicks B J 2017 Using finite element analysis to influence the infill design of fused deposition modelled parts. *Prog Addit Manuf.*
[15] Edward Layer and Krzysztof Tomczyk (Eds.) 2010 *Measurements, Modelling and Simulation of Dynamic Systems* (Springer-Verlag Berlin Heidelberg)
[16] Gavrilin A N, Chuprin A E, Moyzes B B, Halabuzar E A 2014 Land-based sources of seismic signals: *proceedings of the International Conference Mechanical Engineering, Automation and Control Systems (MEACS),* Tomsk, 16-18 Oct. 2014, IEEE, 14823036

http://dx.doi.org/10.1109/MEACS.2014.6986947
[17] Friedman J, Kim H, Mesa O 2014 *Experiments in Additive Clay Depositions*. *In: McGee W., Ponce de Leon M. (eds) Robotic Fabrication in Architecture, Art and Design* (Springer, Cham)
[18] Lenarcic J, Khatib O (Eds.) 2014 Advances in Robot Kinematics. *Springer Cham Heidelberg New York Dordrecht London,*. XII, **561**, 229 DOI 10.1007/978-3-319-06698-1